**1. Michał GOŁĄBEK[1], 2. Tomasz RYMARCZYK[1,2], 3. Piotr BOŻEK[1], 4. Daria STEFAŃCZAK[1,2], 5. Dariusz WÓJCIK[1,2]**

Research & Development Center, Netrix S.A. (1), University of Economics and Innovation (2)
ORCID: 1. 0000-0002-2696-505X; 2. 0000-0002-3524-9151; 3. 0000-0003-4929-1251; 4. 0009-0003-6297-3473; 5. 0000-0002-4200-3432

doi:10.15199/48.2025.03.23

# Portable ultrasound-impedance tomograph for long-term monitoring of the lower urinary tract given electromagnetic compatibility

***Abstract***. *This paper outlines the development process of an ultrasonic tomography device combined with an impedance tomography system designed for monitoring bladder function. By integrating these two tomographic methods, the device provides more accurate urinary tract imaging. The paper presents the results of electromagnetic compatibility tests that were conducted at the accredited Laboratory of Electromagnetic Compatibility (LKE) at Wrocław University of Science and Technology. These tests helped ensure that the device meets industry standards for minimizing electromagnetic interference and maintaining reliable performance.*

***Streszczenie.*** *Niniejsza praca przedstawia proces rozwoju urządzenia do tomografii ultradźwiękowej, połączonego z systemem tomografii impedancyjnej, zaprojektowanego do monitorowania funkcji pęcherza moczowego. W pracy przedstawiono wyniki testów kompatybilności elektromagnetycznej, które zostały przeprowadzone w akredytowanym Laboratorium Kompatybilności Elektromagnetycznej (LKE) na Politechnice Wrocławskiej.* ***(Przenośny hybrydowy tomograf ultradźwiękowo-impedancyjny do monitorowania dolnych dróg moczowych w aspekcie kompatybilności elektromagnetycznej)***

**Keywords:** ultrasound tomography, electroimpedance tomography, electromagnetic compatibility,
**Słowa kluczowe:** tomografia ultradźwiękowa, tomografia impedancyjna, kompatybilność elektromagnetyczna

## Introduction

Urinary tract disorders are common in children, affecting approximately 7-10% of those over the age of 5. The causes can be genetic, environmental, behavioral, or physical [1]. Without proper diagnosis and treatment, these conditions can lead to severe complications, such as urosepsis or kidney damage [2]. Given the complexity of these disorders, accurate diagnosis is essential for effective treatment. The prevalence of bladder dysfunctions, particularly among the pediatric population, calls for innovative diagnostic and therapeutic approaches.

One of the key challenges in developing this system was ensuring electromagnetic compatibility (EMC) while maintaining miniaturization and portability. Achieving EMC was critical, as the device integrates multiple electronic components and generates both ultrasound and electrical signals, which could interfere with each other or external devices. To address this, rigorous EMC testing was conducted, ensuring that the device operates without causing or being affected by electromagnetic interference (EMI). Shielded cables, ferrite filters, and carefully designed circuit layouts were used to minimize emissions and improve immunity to external interference. Additionally, the device was tested at the accredited Laboratory of Electromagnetic Compatibility (LKE) at Wrocław University of Science and Technology to ensure compliance with international standards.

## Hardware

The design of the measuring device for dual diagnosis of the urinary tract is divided into several PCB boards. It consists of the mainboard, four ultrasound measurement cards (UST), one impedance measurement card (EIT), a WiFi communication module, a connectors module, an LED board for operation status indication, and a battery pack.

The mainboard was based on the STM32H7 microcontroller. It supports parallel FMC data transmission operating at 100MHz clock from ultrasonic measurement cards and provides communication with the impedance measurement card using UART and QUAD SPI. In addition, the motherboard has USB 1.0 and USB 2.0 communication ports and a WiFi module for connection to the image reconstruction system. The motherboard also provides the appropriate supply voltage levels to the individual modules.

The four eight-channel UST cards are synchronized for accurate excitation control at 1 ns, featuring a MAX2082 circuit and an Intel FPGA. The EIT card employs 16 textile electrodes with an LTC2203 ADC system (25 msps) for impedance measurements. It uses DAC8830 converters controlled by the FPGA for precise amplitude control.

The urinary tract diagnostic device has a backpack-style housing for comfort, stability, and adjustability. Durable, hygienic materials enable easy cleaning, effectively combining comfort, functionality, and hygiene.

Fig. 1. UST-EIT dual tomograph for bladder monitoring backpack construction

## Measurement sensors

The measurement electrodes must not introduce any interference into the system, nor allow electromagnetic disturbances to escape through them. This makes the construction of the electrodes critically important for accurate EMC testing. Shielded cables were used to ensure the integrity of the measurements and prevent external noise from affecting the results. The careful design and use of shielding in the electrodes and cables are essential for

maintaining the accuracy and reliability of the EMC tests, preventing any loss of the results by external or internal sources of interference.

Fig. 2. UST-EIT dual tomograph for bladder monitoring mounted on a phantom.

Fig. 3. UST-EIT sensors for lower urinary tract measurements.

Ferrite beads were incorporated inside the measurement connectors to protect the device from further interference. These ferrite beads act as additional filters, enhancing high-frequency noise and electromagnetic interference suppression. Their use, alongside shielded cables, provides an extra layer of filtering, ensuring the device remains shielded from internal and external interference throughout the EMC testing process.

**Electromagnetic compatibility test setup**

The imaging device designed for observing the lower urinary tract underwent evaluation at the Accredited Laboratory of Electromagnetic Compatibility, located at Wroclaw University of Science and Technology in Poland. The tests aimed to verify whether the device can be safely used in a “Professional healthcare facility environment and Home Healthcare Environment,” according to PN-EN 60601-1-2 [3]. Initial evaluations took place during the device's development stage to preemptively detect any potential issues and ensure readiness for the last certification assessments.

EMC Immunity Testing:
- Electrical Fast Transient (EFT) immunity tests [4]
- Burst transient immunity tests [4]
- Surge immunity tests [5]
- ESD immunity tests [6]
- Radiated immunity tests [7]
- Conducted immunity test [8]
- Magnetic field immunity test at a frequency of 50Hz [9]
- Voltage Dips, Drops & Interruptions immunity test [10]

Emission tests:
- Conducted emissions tests [11]
- Radiated emissions tests in the frequency range from 30 MHz to 1 GHz, radiated at a distance of 10 meters [12]
- Radiated emissions tests in the frequency range from 1 GHz to 6 GHz, radiated at a distance of 3 meters [12]
- Harmonic tests [13]
- Flicker tests [14]

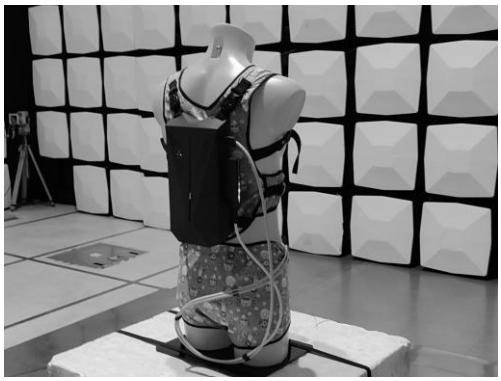

Fig 4. UST-EIT tomograph for monitoring the lower urinary tract mounted on a phantom during radiated immunity and radiated emissions tests in the frequency range 30 MHz – 1GHz.

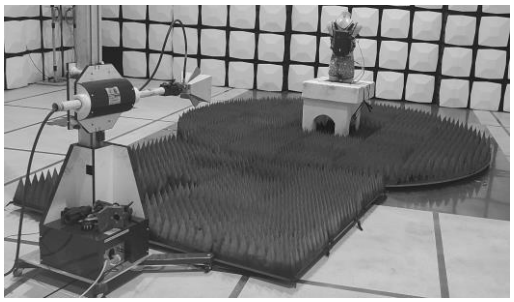

Fig. 5. UST-EIT tomograph for monitoring the lower urinary tract mounted on a phantom during radiated immunity and radiated emissions tests in the frequency range 1 GHz – 6 GHz.

A specialized software program was developed to continuously monitor the device's measurements and battery level to conduct the EMC tests. This program ensured real-time tracking of the device’s performance during the tests, allowing engineers to detect any anomalies or interference as they occurred. Additionally, by monitoring the battery level, the software helped to ensure that power fluctuations did not affect the accuracy of the test results. The combination of real-time measurement and battery management provided a reliable and controlled environment for the EMC testing process, improving the precision and reliability of the outcomes.

**Tests results**

The conducted emissions tests were carried out to evaluate the level of electromagnetic interference (EMI) generated by the device and transmitted through power or signal lines. The test was performed according to the procedure in norms. These tests are critical in determining whether the device meets regulatory limits for EMI, ensuring that it does not cause disruptions in the operation of other electronic systems connected to the same power network. During the testing process, the tomograph was connected to specialized equipment for measurements inside the shielded room [15-20].

This graph in Figure 6 includes all measurement results obtained during the test but shows only the highest level at each frequency. Final measurement results for selected frequencies are presented as a rhombus (measurement using a quasi-peak detector and an average detector). The straight line is the permissible limit for the quasi-peak detector, and the dotted line is the allowable limit for the average detector.

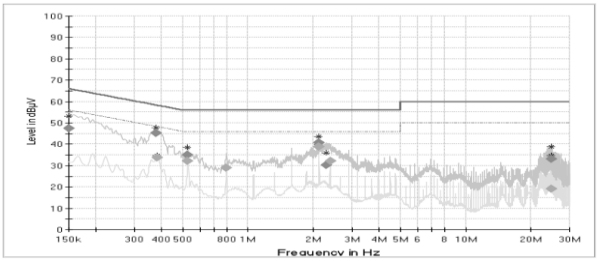


Fig. 6 . Result from the conducted disturbance measurements.

Radiated emissions tests were performed to assess the device's electromagnetic interference (EMI) in the frequency ranges of 30 MHz to 1 GHz and 1 GHz to 6 GHz. These tests are crucial for ensuring that the device does not emit excessive levels of electromagnetic radiation that could interfere with other nearby electronic equipment. In the 30 MHz to 1 GHz range, testing focused on lower-frequency emissions, which are more likely to affect communication systems and other sensitive equipment. Higher-frequency emissions were measured in the 1 GHz to 6 GHz range, which is particularly relevant for devices operating in modern wireless communication bands.

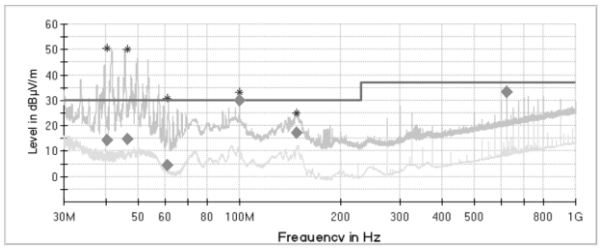


Fig. 7. Result from radiated emissions test in the frequency range from 30 MHz to 1 GHz.

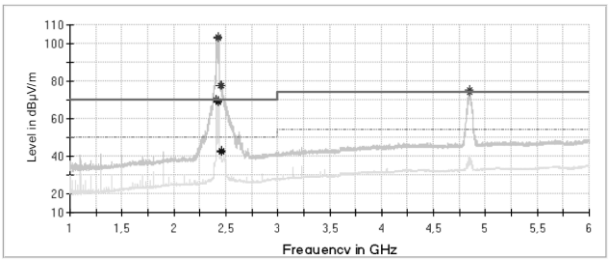


Fig. 8. The result from the radiated emissions test is in a frequency range from 1 GHz to 6 GHz.

Figures 7 and 8 show results for a radiated emission test in the frequency range from 30 MHz to 1 GHz and range from 1 GHz to 6 GHz. The straight line in Figure 7 and Figure 8 shows the limit for the quasi-peak detector, and the dotted line in Figure 8 shows the limits for the average detector. The presented characteristics show that the instantaneous emission levels for several frequencies in the range from 30MHz to 100MHz are exceeded. In such cases, the system selects several points for different frequencies and specific antenna and table settings that require quasi-peak correction.

Radiated immunity tests were conducted to evaluate the device's resistance to electromagnetic interference (EMI) across the frequency ranges of 30 MHz to 1 GHz and 1 GHz to 6 GHz, ensuring its ability to function properly in environments with potential electromagnetic disturbances. These tests are vital for assessing how external electromagnetic fields, such as those emitted by nearby electronic devices, communication systems, or industrial equipment, may affect the device's performance. The primary goal is to confirm that the device can maintain its intended operation without experiencing malfunctions, data corruption, or interruptions when exposed to such interference.

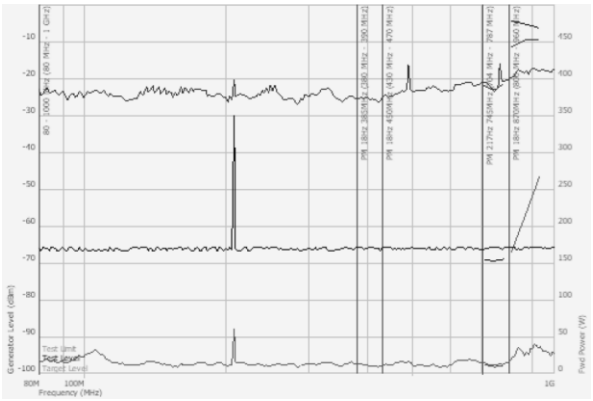

Fig. 9. Levels recorded by the test setup during the radiated, radio frequency, and electromagnetic field immunity test are the SAC for the frequency range from 80 MHz to 1 GHz for vertical polarization of the antenna.

Figure 9 shows levels recorded by the test during the immunity test. The top line represents the applied field strength during the test, indicating a steady electromagnetic field was applied across the frequency range. The middle line represents exposure to the E-field level. The bottom line represents forward power.

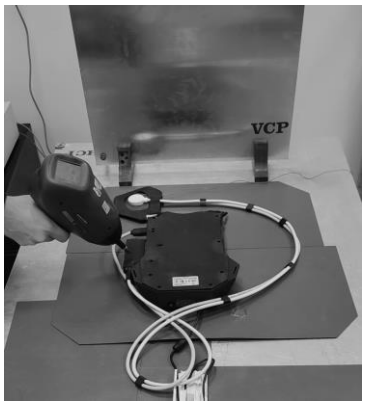


Fig. 10. UST-EIT tomograph during ESD Immunity tests

The device was continuously monitored during the immunity tests to ensure correct functionality. Throughout the exposure to controlled electromagnetic fields, real-time diagnostics were employed to detect any potential malfunctions, performance issues, or deviations from expected operation. This continuous monitoring allowed for immediate identification of any impact the external electromagnetic interference might have on the device's performance, ensuring that it maintained stable and reliable operation throughout the testing process.

Electrostatic discharge (ESD) immunity tests were conducted to assess the device's resilience to sudden electrostatic discharges, which can occur when a charged object comes into contact with the device. These tests are crucial for ensuring that the device can withstand real-world scenarios where electrostatic discharge may occur, such as when a user touches the device after accumulating static electricity.

## Conclusions

Based on the findings, it is clear that best practices in device design for electromagnetic compatibility (EMC) involve continuous testing at each development stage using tools like spectrum analyzers and near-field probes. By identifying high-emission frequencies, appropriate ferrite filters and ceramic capacitors with low ESR can be selected to minimize interference, especially in power supplies and converters. Shielding techniques, such as applying copper layers on both sides of PCBs and placing ferrite beads on long wires, are crucial for reducing electromagnetic emissions and smoothing signal edges. Additionally, effective shielding of enclosures can protect against electromagnetic radiation and electrostatic discharge (ESD), although fully sealed shielding is often challenging due to the need for ventilation.

The study specifically examined the view of electromagnetic compatibility of a mobile ultrasound-impedance tomograph designed for long-term monitoring of the lower urinary tract. In this context, miniaturization and optimization of electromagnetic compatibility were critical factors in ensuring the device's functionality. The combination of ultrasonic tomography (UST) and impedance tomography (EIT) enabled precise imaging while maintaining a compact form factor. Energy efficiency and EMC optimization contributed to the device's practical usability in real-world applications. This innovative solution marks a significant advancement in the diagnosis of urinary tract disorders, particularly in pediatric care, offering new opportunities for precise, non-invasive monitoring and treatment.

***Authors**: Michał Gołąbek M.Sc.,* Research & Development Center *Netrix S.A. Związkowa 26, 20-148 Lublin, E-mail: michal.golabek@netrix.com.pl; Tomasz Rymarczyk, Ph.D. Eng., Faculty of Transport and Computer Science, WSEI University, Projektowa 4, 20-209 Lublin, Poland,* Research & Development Center *Netrix S.A. Związkowa 26, 20-148 Lublin E-mail: tomasz@rymarczyk.com; Piotr Bożek M.Sc.,* Research & Development Center *Netrix S.A. Związkowa 26, 20-148 Lublin, E-mail: piotr.bozek@netrix.com.pl; Daria Stefańczak M.Sc., Faculty of Transport and Computer Science, WSEI University, Projektowa 4, 20-209 Lublin, Poland,* Research & Development Center *Netrix S.A. Związkowa 26, 20-148 Lublin, E-mail: daria.stefanczak@netrix.com.pl; Dariusz Wójcik PhD., Faculty of Transport and Computer Science, WSEI University, Projektowa 4, 20-209 Lublin, Poland,* Research & Development Center *Netrix S.A. Związkowa 26, 20-148 Lublin, E-mail: dariusz.wojcik@netrix.com.pl*

REFERENCES

[1] Nieuwhof-Leppink A.J., Schroeder R.PJ., Van de Putte E.M., De Jong T.P.V.M., Schappin R., Daytime Urinary Incontinence in Children and Adolescents, *Lancet Child Adolesc Health*, 3 (2019), No.7, 492-501

[2] Elale A.K., Manilal A., Tadesse D., Seid M., Dubale, A., Magnitude and Associated Factors of Bacterial Urinary Tract Infections among Paediatric Patients in Arba Minch, Southern Ethiopia, *New Microbes New Infect*, 51 (2023), No. 6, 101083

[3] PN-EN 60601-1-2:2015-11 (EN 60601-1-2:2015) Standard Medical Electrical Equipment - Part 1-2: General Requirements for Basic Safety and Essential Performance - Collateral Standard: Electromagnetic Disturbances - Requirements and Tests.

[4] PN-EN 61000-4-4:2013-05 (EN 61000-4-4:2012) Standard Electromagnetic Compatibility (EMC) - Part 4-4: Testing and Measurement Techniques - Electrical Fast Transient/Burst Immunity Test.

[5] PN-EN 61000-4-5:2014-10 + A1:2018-01 (EN 61000-4-5:2014 + A1:2017) Standard Electromagnetic Compatibility (EMC) - Part 4-5: Testing and Measurement Techniques - Surge Immunity Test.

[6] PN-EN 61000-4-2:2011 (EN 61000-4-2:2009) Standard Electromagnetic Compatibility (EMC) - Part 4-2: Testing and Measurement Techniques - Electrostatic Discharge Immunity Test.

[7] PN-EN 61000-4-3:2021-06 (EN IEC 61000-4-3:2020) Standard Electromagnetic Compatibility (EMC) - Part 4-3 : Testing and Measurement Techniques - Radiated, Radio-Frequency, Electromagnetic Field Immunity Test.

[8] PN-EN 61000-4-6:2014-04 (EN 61000-4-6:2014) Standard Electromagnetic Compatibility (EMC) - Part 4-6: Testing and Measurement Techniques - Immunity to Conducted Disturbances, Induced by Radio-Frequency Fields.

[9] PN-EN 61000-4-8:2010 (EN 61000-4-8:2010) Standard Electromagnetic Compatibility (EMC) - Part 4-8: Testing and Measurement Techniques - Power Frequency Magnetic Field Immunity Test.

[10] PN-EN 61000-4-11:2020-11 (EN IEC 61000-4-11:2020) Standard Electromagnetic Compatibility (EMC) - Part 4-11: Testing and Measurement Techniques - Voltage Dips, Short Interruptions and Voltage Variations Immunity Tests for Equipment with Input Current up to 16 A per Phase.

[11] PN-EN 55016-2-1:2014-09 + A1:2017-12 (EN 55016-2-1:2014 + A1:2017) Standard Specification for Radio Disturbance and Immunity Measuring Apparatus and Methods - Part 2-1: Methods of Measurement of Disturbances and Immunity - Conducted Disturbance Measurements.

[12] PN-EN 55016-2-3:2017-06 + A1:2020-01 (EN 55016-2-3:2017 + A1:2019) Standard Specification for Radio Disturbance and Immunity Measuring Apparatus and Methods - Part 2-3: Methods of Measurement of Disturbances and Immunity - Radiated Disturbance Measurements.

[13] PN-EN 61000-3-2:2019-04 + A1:2021-08 (EN IEC 61000-3-2:2019 + A1:2020) Standard Electromagnetic Compatibility (EMC) - Part 3-2: Limits - Limits for Harmonic Current Emissions (Equipment Input Current ≤16 A per Phase.

[14] PN-EN 61000-3-3:2013-10 + A1:2019-10 + A2:2022-04 (EN 61000-3-3:2013 + A1:2019 + A2:2021) Standard Electromagnetic Compatibility (EMC) - Part 3-3: Limits - Limitation of Voltage Changes, Voltage Fluctuations and Flicker in Public Low-Voltage Supply Systems, for Equipment with Rated Current ≤16 A per Phase and Not Subject to Conditional Connection.

[15] Krawczyk A. Korzeniewska E., Some Aspects of Electromagnetic Field Shielding. Przeglad Elektrotechniczny 99 (2023), No.3, 128-131

[16] Kozłowski E., Borucka A., Oleszczuk P., Jałowiec T., Evaluation of the maintenance system readiness using the semi-Markov model taking into account hidden factors, *Eksploatacja i Niezawodność – Maintenance and Reliability,* 25 (2023) ;No. 4, 172857

[17] Kłosowski G, Rymarczyk T, Niderla K, Kulisz M, Skowron Ł, Soleimani M. Using an LSTM network to monitor industrial reactors using electrical capacitance and impedance tomography – a hybrid approach, *Eksploatacja i Niezawodnosc – Maintenance and Reliability*, 25 (2023). No.1

[18] Król, K., Rymarczyk, T., Niderla, K., & Kozłowski, E., Sensor platform of industrial tomography for diagnostics and control of technological processes. *Informatyka, Automatyka, Pomiary W Gospodarce I Ochronie Środowiska,* 13 (2023), No.1, 33–37

[19] Kulisz M., Kłosowski G., Rymarczyk T., Hoła A., Niderla K., Sikora J., The use of the multi-sequential LSTM in electrical tomography for masonry wall moisture detection*, Measurement,* 234 (2024) 114860.

[20] Kulisz M, Kłosowski G, Rymarczyk T, Słoniec J, Gauda K, Cwynar W. Optimizing the Neural Network Loss Function in Electrical Tomography to Increase Energy Efficiency in Industrial Reactors*. Energies,* 17 (2024); No. 3, 681